

- (4) Šolc, K. *J. Polym. Sci., Polym. Phys. Ed.* **1982**, 20, 1947.
- (5) Yang, Y. C.; Šolc, K. *Polym. Prepr. (Am. Chem. Soc., Div. Polym. Chem.)* **1987**, 28 (2), 246.
- (6) Šolc, K. *Macromolecules* **1986**, 19, 1166.
- (7) The term *critical line* as used in this report has a generic meaning of a locus of critical points in any coordinates. Traditional interpretation would be the critical temperature plotted as a function of critical composition for a given ternary system [coded as $T(w_2)$], but it could also be $\bar{g}(w_2)$ (since \bar{g} is a well-defined function of temperature) or, e.g., $\xi^2(w_2)$ (where the critical value of ξ^2 is defined from eq 1-3). An attached qualifier specifies which critical line is concerned.
- (8) See, e.g.: Šolc, K.; Koningsveld, R. *J. Phys. Chem.* **1985**, 89, 2237.
- (9) Šolc, K.; Kleintjens, L. A.; Koningsveld, R. *Macromolecules* **1984**, 17, 573.
- (10) Šolc, K.; Battjes, K. *Macromolecules* **1985**, 18, 220.
- (11) Scott, R. L. *J. Chem. Phys.* **1949**, 17, 279.

Comparison of the Translational Diffusion of Large Spheres and High Molecular Weight Coils in Polymer Solutions

Wyn Brown* and Roger Rymdén

*Institute of Physical Chemistry, University of Uppsala, Box 532, 751 21 Uppsala, Sweden.
Received May 19, 1987; Revised Manuscript Received September 12, 1987*

ABSTRACT: The translational diffusion of large stearic acid coated silica spheres ($R_H = 1595 \text{ \AA}$) and high molecular weight polystyrene (PS) fractions in poly(methyl methacrylate) (PMMA) solutions has been examined by using dynamic light scattering (QELS) over the dilute/semidilute concentration ranges of the latter polymer. When the PMMA concentration is normalized by the overlap concentration, C^* , the reduced diffusion coefficient (D/D_0) for the sphere is a universal function of C_{PMMA} . A similar observation applies to the data for the PS fractions. This is in accord with scaling predictions. The product $D_{\text{SiO}_2}\eta$ is a constant, independent of both C_{PMMA} and M_{PMMA} , where η is the macroscopic solution viscosity of the medium. Thus the Stokes-Einstein equation applies. In contrast $D_{\text{PS}}\eta$ is an increasing function of C_{PMMA} and this trend is more pronounced at higher M_{PMMA} . Although the Stokes-Einstein mechanism is assumed to also apply with linear probe chains, it is concluded that there may be a significant coupling of the dynamics of the probe chain and those of the network polymer.

Introduction

Recently, considerable attention has been focused on the single-chain diffusion of a linear polymer in a matrix of a second polymer at semidilute concentrations. One approach has been to use dynamic light scattering (QELS) from isorefractive ternary solutions: the host polymer is index matched¹⁻¹³ to a simple solvent and the probe polymer (at very low concentration and having good optical contrast) studied as a function of molecular weight and matrix polymer concentration. This is the so-called "optical-labeling" technique where it is assumed⁵ that QELS monitors self-diffusion at a low but finite concentration of the test chain. (It will differ from the more strictly considered self-diffusion coefficient of a spin-labeled individual in a sea of otherwise identical chains as determined, for example, in pulsed field gradient NMR, to the extent that there may be significant chemical and size differences between probe and host chains.)

Recent examples of the optical-labeling approach include use of polystyrenes (PS) as the probe chain in transient networks of poly(methyl methacrylate) (PMMA),^{2,3,11,12} index matched with toluene or benzene, or poly(vinyl methyl ether) (PVME) in toluene^{6,8} or *o*-fluorotoluene.^{4,7,9,10} Chu and co-workers¹³ have ingeniously included a second simple solvent so that the contrast can be also varied to match either the PS or PMMA.

For a recent discussion of such investigations one may refer to the paper of Numasawa et al.¹¹ From the accumulated data in the above studies, it is apparent that translational diffusion of a linear probe chain in the network of the second chain may proceed by two main processes.

1. **Stokes-Einstein (S-E) diffusion** which is governed by the macroscopic viscosity (η) of the host solution and the hydrodynamic radius (R_H) of the probe chain is given according to

$$D_s = kT/6\pi\eta R_H \quad (1)$$

Due to hydrodynamic screening effects, this process may become independent of the molecular weight of the guest chain and also exhibit extreme dependence on the concentration of the host polymer.

2. **Reptation** is the process whereby the probe chain diffuses along a fictive tube formed by the topological constraints of the surrounding chains. In a good solvent, this model leads to the scaling prediction:¹⁴

$$D_s \sim M^{-2}C^{-1.75} \quad (2)$$

Thus D_s should be strongly dependent on the chain length (guest polymer) and also the concentration (C) of the matrix polymer. D_s may also become independent of the molecular weight of the matrix polymer, however. Recent discussions have centered on modifying effects (the "noodle" effect¹⁵ and constraint release^{16,17}) which model contributions from surrounding chains, and these lead to modifications in the scaling expression.

Although the above remarks center on the results obtained in ternary systems, we note the possible presence in binary systems of translational motion in semidilute solutions.²⁰⁻²³ Thus even in good solvents the photocount autocorrelation function may be bimodal^{20,42,43} (gel mode accompanied by translation). As the solvent quality is reduced, toward Θ conditions an additional very slow mode becomes evident in the CONTIN inversion of the time correlation function and this may be attributed to a structural relaxation and/or motions of clusters of chains.⁴⁴⁻⁴⁷ In the ternary systems the main processes (1 and 2 above) play different relative roles depending on the concentration of the matrix polymer as well as the relative sizes of host and matrix chains. S-E diffusion apparently extends throughout much of the usually defined semidilute region^{5,8-11,48} up to the point where extensive interpen-

tration of the coils has occurred. Wheeler et al.¹⁰ suggest that a concentration in excess of the critical concentration for entanglement⁴¹ (C_E) is a minimum requirement for reptation to become the dominant mechanism. The hypothesized crossover from S-E motion to reptation depends on the relative molecular weights of guest and host chains^{5,8,11} such that at lower molecular weights of the probe chain the crossover is displaced to lower matrix polymer concentration. Owing to experimental curtailments, most investigations of ternary polymer systems have spanned the crossover region where processes 1 and 2 both participate. As mentioned above, a mixture of transport mechanisms is also prevalent in binary systems and this is a probable source of the conflicting results reported for scaling exponents determined for the effective diffusion measured by using pulsed field gradient NMR²⁴ and forced Rayleigh scattering experiments.^{25,26} Thus in spite of determined efforts, it has been difficult to unequivocally establish the exponents predicted in eq 2. Some workers observe continuously variable slopes²⁵ in the log-log plots of D_s versus C . This may be understood by changes in the relative weighting of S-E diffusion and reptation which will depend on factors such as the solvent quality and the molecular weight of the probe chain. Thus the oversimplified view of the dynamical processes as occurring in a hypothetically homogenous transient gel and being restricted only to a cooperative gel mode and reptation leads to interpretative problems. There is increasing evidence³²⁻³⁴ that polymer coils (even in the binary solution) only partially interpenetrate and this leads to freedom for other types of motion (e.g., S-E diffusion and cluster translation) throughout the semidilute region. Daoud and de Gennes⁴⁰ have treated the dynamical behavior of melts and point out the dominant role played by S-E diffusion when the guest chain is very large compared to chains of the host polymer. However, it is apparent that S-E diffusion in semidilute systems needs further elucidation. Thus the description of sphere transport in polymer solutions has been the source of some ambiguity as regards possible limitations to the applicability of eq 1. Phillies et al.^{18,19} have observed that latex particles diffusing in aqueous polymer solutions only obey eq 1 when the matrix polymer is of low molecular weight ($M \leq 7000$) and that, in general, the deviations from this equation become large when the matrix molecular weight is high.

We have chosen here to examine the asymptotic region of large probe particle size ($R_H \gg \xi$) where ξ is the static correlation length defining the average mesh size of the transient network formed by the host chains. The experiments described compare (1) the translational diffusion of large SiO₂ spheres, stabilized in organic solvents by a covalently attached layer of stearic acid, in good solvent solutions of PMMA and (2) the diffusion of very high molecular weight PS fractions ($\bar{M}_w = 8 \times 10^6$ and 15×10^6) in solutions of the same fractions of PMMA at semidilute concentrations. It will be shown that while the spheres are well-behaved in following eq 1, the linear probe chains adopt a much more complex pattern due to their ability to participate in cooperative network motions.

Experimental Section

Sterically stabilized silica particles were a kind gift from Dr. K. de Kruif, University of Utrecht, The Netherlands. The stabilizing moiety is a layer of terminally grafted C₁₈H₃₇-O-Si. The synthesis has been described by Vrij et al.³¹ The hydrodynamic radius of the particles is 1595 Å as determined by dynamic light scattering in chloroform suspension. While the PMMA polymer and chloroform are not isorefractive, the scattering from the spheres completely dominated the scattering behavior and

the contribution from the polymer was less than 1% of the total.

Polystyrene samples were obtained from Toya Soda Ltd., Tokyo: $\bar{M}_w = 2.95 \times 10^6$ ($\bar{M}_w/\bar{M}_n = 1.06$); $\bar{M}_w = 8 \times 10^6$ ($\bar{M}_w/\bar{M}_n = 1.08$); $\bar{M}_w = 15 \times 10^6$ ($\bar{M}_w/\bar{M}_n = 1.30$). The solvents were spectroscopic grade from Merck, Darmstadt.

Poly(methyl methacrylate) samples were reprecipitated materials, subsequently freeze-dried. The molecular weights (intensity light scattering) and intrinsic viscosities are as follows:

$\bar{M}_w \times 10^5$	$[\eta]/\text{dL}\cdot\text{g}^{-1}$ (chloroform, 25 °C)
4.45	1.64
2.68	1.05
1.63	0.85
1.01	0.45

PMMA fractions of higher molecular weight were obtained from Pressure Chemical Co., Pittsburgh, PA: 6.97×10^5 and 1.426×10^6 , both having $\bar{M}_w/\bar{M}_n = 1.09$.

Viscosity measurements were made in a calibrated Ubbelohde capillary viscometer at 25 °C, without shear corrections.

Quasielastic light scattering (QELS) measurements were made by using the apparatus and techniques described earlier.²⁰⁻²² Filtered (0.5- μm Fluoropore filters from Millipore) stock solutions of the sphere (or polystyrene) solutions at high dilution were prepared. These were mixed by volume with the appropriate quantity of the filtered PMMA solutions (0.22 μm Fluoropore filters) and allowed to equilibrate prior to measurement. All determinations were made at 25 °C and initially over a range of angles to ascertain q^2 dependence of the relaxation rate.

The autocorrelator used was a multi-tau model (ALV-Langen, FRG), with 23 simultaneous sampling times covering typically the lag-time range 1 μs to 1 min. Only a single relaxational decay was evident. However, all QELS runs were routinely processed by using two- and three-parameter cumulant fits and also by discrete multiexponential fits. Both with the SiO₂ spheres and the high molecular weight polystyrenes there was a small amount ($\leq 2\%$) of a considerably faster component which was easily separable. Since the decay time of the fast contaminant was more than $10\times$ faster than that of the main component, use of the cumulants method would have introduced significant error. Use of the multi-tau correlator has greatly facilitated the determination of decay time spectra with acceptable precision by extension of the time base by several powers of 10. D values down to $10^{-14} \text{ m}^2 \text{ s}^{-1}$ have been routinely determined at the highest concentrations—see, for example, Figure 5.

Results and Discussion

A. Diffusion of SiO₂ Spheres in PMMA Solutions.

Measurements of the diffusion of stearic acid coated SiO₂ spheres were made in PMMA solutions in chloroform, the concentration range covering both dilute and semidilute ranges. Chloroform was used as the medium since it is a suitably good solvent both for the coated spheres and the PMMA. Although the PMMA and solvent are not precisely index matched ($n_D(\text{CHCl}_3) = 1.4459$ and $n_D(\text{PMMA}) = 1.4947^{28}$), the scattering from the large SiO₂ spheres ($\text{rad} = 1595 \text{ \AA}$) completely dominates the scattering pattern ($\geq 98\%$ of the intensity from the SiO₂ particles).

It was first established that the effective diffusion coefficient ($D = \bar{\Gamma}_1/q^2$, where $\bar{\Gamma}_1$ is the initial decay rate and q is the scattering vector, $q = (4\pi/\lambda) \sin(\theta/2)$) was independent of angle in the range 20–120°. Thereafter, measurements were made at $\theta = 70^\circ$. The concentration of SiO₂ particles was maintained at $5 \times 10^{-4} \text{ g mL}^{-1}$ which fell in the range where no concentration dependence of the diffusion coefficient was observed. Thus the determined quantity may be taken to approximate the self-diffusion coefficient for the "labeled" particle, as previously done.⁵⁻¹⁰

It was noted that the relative variance from the cumulant evaluation of data for the particles suspended in the pure solvent was small (≤ 0.05), indicating that the sphere suspension was essentially monodisperse. In measurements on the ternary systems, bimodal fitting was used to separate the small contribution to the autocorrelation

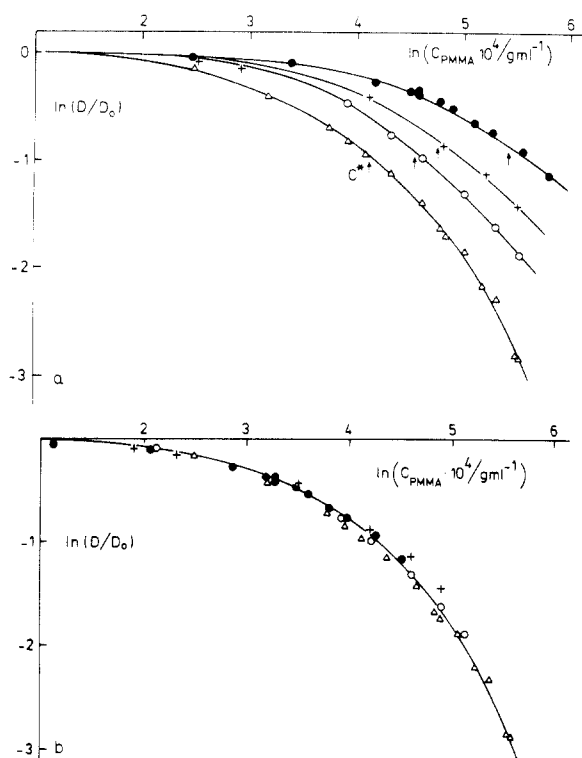


Figure 1. Reduced diffusion coefficient for SiO_2 spheres in PMMA solutions (D_0 is the D value in the absence of PMMA) in a double-logarithmic plot where C^* ($=1/[\eta]$) indicates PMMA overlap concentrations. M_{PMMA} : (●) 1.01×10^5 ; (+) 1.63×10^5 ; (○) 2.68×10^5 ; (Δ) 4.45×10^5 . The lower diagram (insert) is obtained by horizontal displacement of the data (relative to those for $\bar{M}_w = 4.45 \times 10^5$) in the main figure by an amount equal to the difference in the C^* values. Data are in chloroform at 25 °C.

function from the PMMA. This procedure has been described previously.²¹ Plots of $\ln(D/D_0)$ versus $\ln C_{\text{PMMA}}$ are shown in Figure 1 for four molecular weights of PMMA. (The C^* values indicated are for PMMA and have been approximated as $1/[\eta]$. This measure of the overlap concentration has been shown experimentally²⁹ to provide a consistent estimate.) The quantity $\ln(D/D_0)$ is seen to depend significantly on M_{PMMA} : at a concentration, $C_{\text{PMMA}} = 1.5\%$ we find $D/D_0 \sim M^{-0.88}$. We note that Kim et al.²⁶ also found a substantial molecular weight dependence for the labeled chain in forced Rayleigh scattering (FRS) measurements in the binary system PS/toluene. This dependence only vanished when $M_{\text{matrix}} \geq (3-5)M_{\text{guest}}$. However, horizontal displacement of the curves in Figure 1a by an amount equal to the difference in C^*_{PMMA} values to give comparable length scales leads to a universal curve as illustrated in the insert. This finding agrees with the predictions of scaling theory¹⁴ for which diffusion coefficients for samples of different molecular weight should follow a universal curve which is only a function of the variable C/C^* .

The concentration range of the PMMA has been maintained low ($\leq 5\%$ PMMA) so that the monomeric friction coefficient is essentially constant.³⁶ This will not be the case when the concentration exceeds 10–15%, however.²⁶ Figure 2 shows that the product $(D\eta)$ is strictly independent of both the PMMA concentration and its molecular weight. This is the expected result when the probe particle is very much larger than the correlation length (mesh size), ξ , characterizing the polymer network.³⁰ The value of $(D\eta)$ for SiO_2 in the pure solvent also equals that found in the PMMA solutions. The dynamic correlation length (ξ_H) in the PMMA solutions was determined in separate experiments on solutions of PMMA ($\bar{M}_w = 4.45$

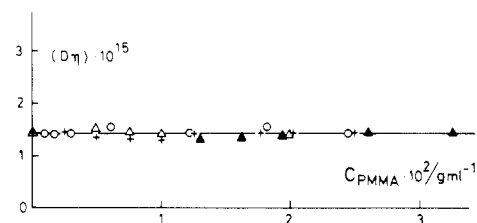


Figure 2. Product of D_{SiO_2} and the macroscopic viscosity of the PMMA solutions as a function of PMMA concentration in toluene at 25 °C. (M_{PMMA}): (Δ) 1.01×10^5 ; (○) 1.63×10^5 ; (▲) 2.68×10^5 ; (+) 4.45×10^5 .

$\times 10^5$). ξ_H ranges between 270 Å at 0.04% PMMA and 35 Å at 4% PMMA. Since the ratio of the hydrodynamic screening length to the static length is close to 2 in a good solvent,²⁹ it is clear that the probe particle size greatly exceeds the network dimension. Thus when $R_H \gg \xi$, the matrix may be considered as a continuum relative to the particle and the decrease in D_{sphere} should be mirrored by the increase in the macroscopic solution viscosity with matrix polymer concentration as predicted by Langevin and Rondelez.³⁰

Sphere self-diffusion has earlier been extensively studied (see, for example, ref 18 and 19), although almost entirely in aqueous polymer solutions and charge-stabilized latex spheres have been employed as the probe particle. The results of these studies are ambiguous, however, since it was found that large discrepancies exist when eq 1 containing the macroscopic viscosity was used to predict the value of R_H . The R_H values are too small by as much as several orders of magnitude. We have made a similar observation³⁹ for the apparent hydrodynamic radius of similar latex particles in solutions of water-soluble cellulose derivatives: R_H exhibits an initial increase with polymer concentration (probably due to the thickness of the adsorbed layer of polymer at the latex interface) followed by a monotonic decrease in R_H to well below the radius of the isolated sphere at infinite dilution.

We consider this phenomenon to most likely be rooted in perturbation of the particle diffusion by the motions of the polymer network mediated by the pronounced dipolar interactions in such systems. In comparison with the well-behaved Stokes–Einstein character of the transport of the spheres currently investigated in a good solvent system, we conclude that when serious departures from eq 1 are observed, this is probably indicative of the influence of the network dynamics being imprinted on those of the probe. This cooperative effect would be expected to depend on the polymer concentration and also probe radius as observed by Phillies et al.^{18,19} Thus, Phillies et al.¹⁸ observed an increasing deviation from the Stokes–Einstein equation both with increasing concentration and latex sphere size in the poly(ethylene oxide) aqueous system. Some of the earlier conclusions which have been drawn regarding probe dynamics in polymer solutions may thus be erroneous on this account. Below it is noted that a similar cooperative effect is also met with when the probe particle is a linear chain instead of a hard sphere.

Altenberger et al.³⁵ have used a mean-field approach to analyze the influence of hydrodynamic screening on particle dynamics in a gel network composed of rigid segments. They predict that when the matrix polymer chains are long and well-entangled, such that several blobs¹⁴ are formed from each chain, the reduced mobility of the particle should not depend on the chain mass and should also become independent of the radius of the mobile particle. We agree on the first finding, although the unavailability of SiO_2 spheres of different radius precluded

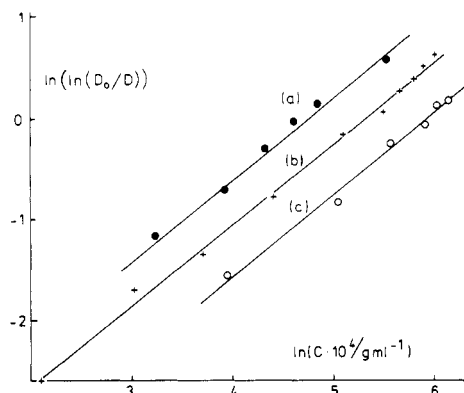


Figure 3. Determination of the exponent in eq 3. The data are for D_{SiO_2} values reduced by D_0 at 25 °C. (a) 4.45×10^5 , (b) 2.68×10^5 , and (c) 1.01×10^5 are PMMA molecular weights.

Table I

Dilute Solution Dimensions for Polystyrenes in Toluene

molecular wt/ 10^6	$D_0 \times 10^{12}/\text{m}^2 \text{ s}^{-1}$	$R_H/\text{\AA}^a$	$R_g/\text{\AA}^b$
15	3.1	1270	2255
8.0	4.3 ₈	895	1550
2.95	8.1	485	855
1.26	12.65	310	515

^a Using eq 1 with D_0 values. ^b $R_g = 0.1212M_w^{0.596}/\text{\AA}^{37}$

examination of the second point. The suggested proportionality of D/D_0 to $\phi^{1/2}$, where ϕ is the volume fraction of network polymer, has not been found to adequately describe the present data. Moreover, Altenberger et al.³⁵ do not predict that D/D_0 is a function of C/C^* as is shown by the present data.

The stretched exponential form

$$D/D_0 = \exp(-AC^\nu) \quad (3)$$

does, however, provide a good fit and this method of data presentation has been extensively used by Phillies et al.; see, for example, ref 18 and 19. With the present data we find $\nu = 0.91$ (Figure 3).

We note that Phillies³⁸ has recently presented a justification for an equation of the form of eq 3; although, as pointed out by Altenberger,³⁵ such a description has not yet resulted in a deeper understanding of the underlying mechanism of diffusion of the probe.

B. Diffusion of Linear Polystyrenes in PMMA Solutions. An analogous series of measurements to those on the SiO_2 spheres were made by using high molecular weight, essentially monodisperse, PS fractions in PMMA solutions. The solvent used in these experiments was toluene (having approximately the same thermodynamic quality for PS as chloroform) since toluene provided almost perfect refractive index matching with PMMA. This was essential since the two polymers were of comparable scattering power, in contrast to the SiO_2 sphere/polymer system. Dilute solution values of the dimensions of the PS fractions are listed in Table I. The experimental values of D_0 , obtained from measurements in dilute toluene solution in the absence of PMMA, are given with the corresponding hydrodynamic radii by using eq 1 and radii of gyration obtained by using the relationship of Miyaki et al.³⁷ The D_0 values fit the function $D_0 \sim M^{-0.59}$. The measurements were made by using a PS concentration of $2.5 \times 10^{-4} \text{ g mL}^{-1}$, thus ensuring that single-chain translation of the PS was measured. A measurement angle of 20° was used after it had been established that the effective diffusion coefficient $D = \Gamma_1/q^2$ was constant over the angular region of interest; see Figure 4. The autocorrelation

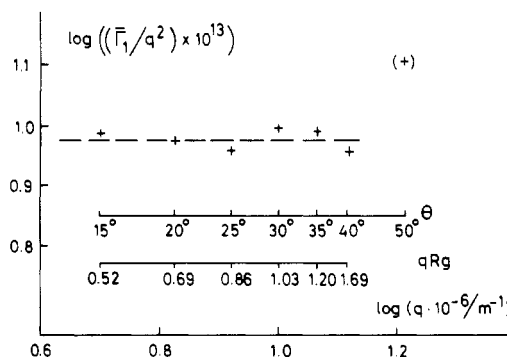


Figure 4. Plots of the effective diffusion coefficient versus $\log q$ (the scattering vector) for PS ($\bar{M}_w = 2.95 \times 10^6$) in PMMA ($\bar{M}_w = 4.45 \times 10^6$) solution ($C_{\text{PMMA}} = 2.04\%$). The angular range and the corresponding qR_g values are indicated, where R_g is the radius of gyration of the PS sample (Table I).

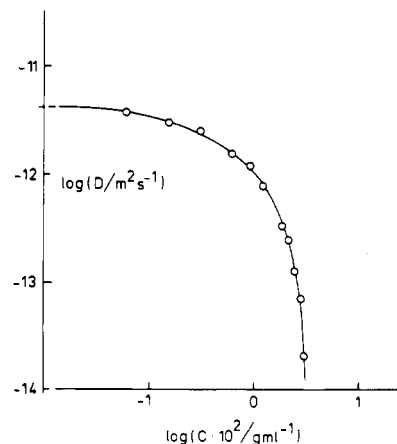


Figure 5. Diffusion coefficients for PS ($\bar{M}_w = 8 \times 10^6$) in toluene solutions of PMMA ($\bar{M}_w = 1.426 \times 10^6$) as a function of PMMA concentration.

functions were bimodal, usually with less than 2% of a component having a decay rate more than 10 times faster than the major component and which presumably derived from internal relaxations.

The major component is considered to represent center of mass displacements of the whole PS coil (S-E diffusion) in the PMMA solutions. Diffusion coefficients for PS ($\bar{M}_w = 8 \times 10^6$) in the PMMA fraction with $\bar{M}_w = 1.4 \times 10^6$ are shown in Figure 5. D has decreased by more than two powers of 10 at the highest concentration: $C_{\text{PMMA}} = 3\%$. Data for the reduced diffusion coefficient of this fraction of PS in solutions of various molecular weight fractions of PMMA in toluene are shown in Figure 6. The dependence of D/D_0 for PS on C_{PMMA} shows a progressive increase with M_{PMMA} . At $C_{\text{PMMA}} = 1.5\%$ this is given by $D/D_0 \sim M_{\text{PMMA}}^{-0.5}$. As in Figure 1b, horizontal displacement of the four curves for the lower molecular weights by an amount equal to the differences in the C^* values yields a universal curve as is shown in the insert. Thus this conforms to the pattern of the data for the SiO_2 spheres and is in line with the expectation from scaling theory.¹⁴ We note that Kim et al.²⁶ also find scaling with C/C^* in semidilute binary solutions over a broad interval of molecular weight.

The role of the molecular weight of the guest polymer was also examined by using PS fractions with $\bar{M}_w = 1.26 \times 10^6$, 2.95×10^6 , 8×10^6 , and 15×10^6 in conjunction with a PMMA fraction with $\bar{M}_w = 4.45 \times 10^5$. For the three higher molecular weights, the curves for $\ln D/D_0$ versus $\ln C_{\text{PMMA}}$ (see the data in Figure 7) were approximately superimposable. Thus the molecular weight independence

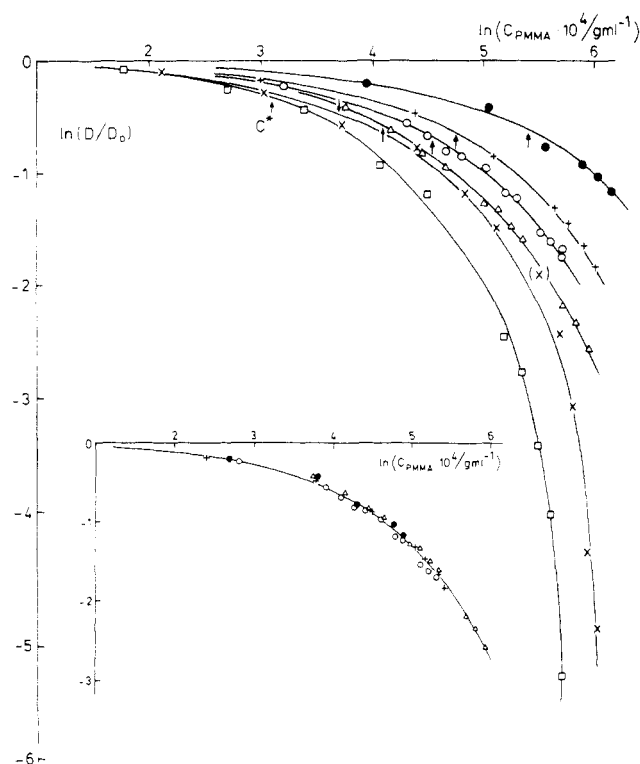


Figure 6. Reduced diffusion coefficient of polystyrene ($\bar{M}_w = 8 \times 10^6$) in PMMA solutions of different molecular weight as a function of C_{PMMA} in a log-log plot. M_{PMMA} : (●) 1.01×10^5 ; (+) 1.63×10^5 ; (○) 2.68×10^5 ; (Δ) 4.45×10^5 ; (×) 6.97×10^5 ; (□) 1.426×10^6 . The plot in the insert is for the four lower PMMA fractions where the data have been displaced horizontally (relative to those for $M_{\text{PMMA}} = 4.45 \times 10^5$) by an amount equal to the difference in the corresponding C^* values. This diagram is analogous to that in Figure 1b. Data are in toluene at 25 °C.

extends both to the matrix polymer (when normalized with C^*) and to the guest polymer. This conclusion that the reduced mobility does not depend on the molecular weight of the guest chain, when of sufficient length, is also supported by the data of Numasawa et al.¹¹ the molecular weight dependence of D_{probe} increases strongly, however, with decreasing coil size of the probe molecule. This conclusion falls into line with the results of the treatment of Altenberger et al.³⁵ who considered the random Brownian motion of the particle through a gel network which generates hydrodynamic screening: the reduced hydrodynamic mobility eventually becomes independent of the radius of the mobile particle.

While the relative intensity of the fast component was almost insignificant with the higher molecular weight PS fractions, it was significant for the fraction of $\bar{M}_w = 1.26 \times 10^6$, the relative intensity increasing to about 30%. Such bimodality was also noted by Nemoto et al.⁶ and Chu et al.¹³ and was then interpreted as deriving from the coupling of the dynamics of the probe chain with those of the matrix polymer. Such an effect should be emphasized with shorter chains due to the more effective interpenetration of the coils. In an analogous system, Martin^{5,8} presents data supporting a crossover from S-E diffusion to reptation and this, as would be expected, occurs at a lower concentration for a lower molecular weight guest chain.

It is noted that a tangent with slope = -1.75 may be drawn with reasonable agreement with the data points for the normalized curve (insert to Figure 6) at the highest concentrations. However, it is also apparent from the data for the two highest molecular weight PMMA fractions in the main diagram that the tangential slope continues to increase strongly and without apparent limit (see also ref

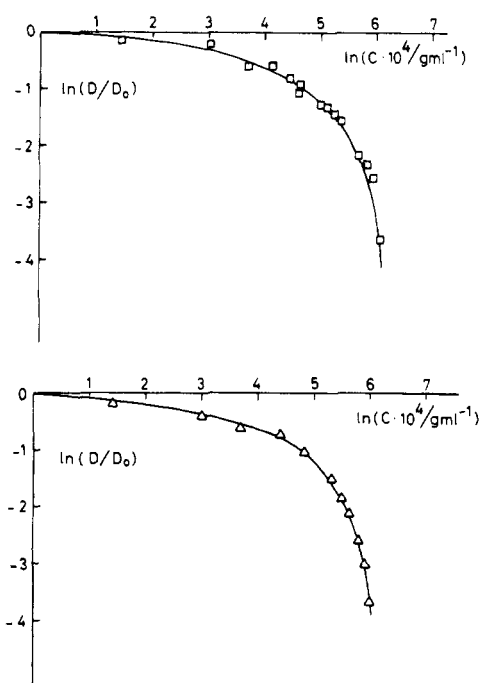


Figure 7. Reduced diffusion coefficients for (a) PS (3×10^6) and (b) PS (15×10^6) in PMMA ($\bar{M}_w = 4.45 \times 10^5$). These plots superimpose within experimental error with the corresponding plot for PS ($\bar{M}_w = 8 \times 10^6$) shown in the preceding diagram (Figure 6).

25). At a matrix concentration of 3% (PMMA, $\bar{M}_w = 1.4 \times 10^6$) the self-diffusion coefficient for PS ($\bar{M}_w = 8 \times 10^6$) is almost immeasurably slow in the QELS experiment ($D \approx 10^{-14} \text{ m}^2 \text{ s}^{-1}$; see Figure 5). We also note that with this PS molecular weight the autocorrelation function is still a clean single exponential ($\geq 99.5\%$) and there is no indication that the crossover to a reptative mechanism is being approached. The data are thus consistent with the general picture of Martin,^{5,8} indicating that reptation should only be anticipated with significant amplitude at substantially higher PMMA concentrations than used here. Figure 8a illustrates the dependence of the product $D\eta$ on PMMA concentration and Figure 8b shows the influence of PMMA molecular weight on PS diffusion. $D\eta$ increases with C_{PMMA} except for the fraction of lowest molecular weight. This trend has previously been noted by Numasawa et al.¹¹ A possible cause is a contraction of the guest polymer coil in the presence of the host chains, although the assumption is usually made implicitly that the polymers are miscible on the molecular level and that the dynamical behavior resembles that in the binary polymer-solvent system. Indeed, Wheeler et al.¹⁰ suggest that the PS coil contracts to θ dimensions in the presence of PVME. On the other hand, Numasawa et al.'s measurements¹¹ of the PS radius of gyration in PMMA solutions show that this effect is probably small in the present system and, in any event, the change in $D\eta$ is too large to be explained entirely by a coil contraction even to its θ dimensions; see Figure 8c. The increase in $D\eta$ most likely does not derive from incipient reptation since when the latter contributes significantly, the autocorrelation function can be expected to deviate strongly from a single exponential.

Figure 8c shows how the apparent hydrodynamic radius would vary if the divergence from the Stokes' radius at $C \rightarrow 0$ were attributed to coil contraction only. A more likely source of the increase in $D\eta$ is probably a coupling of the PS dynamics with those of the matrix polymer network^{6,13} owing to the physical interpenetration of their coils. Such

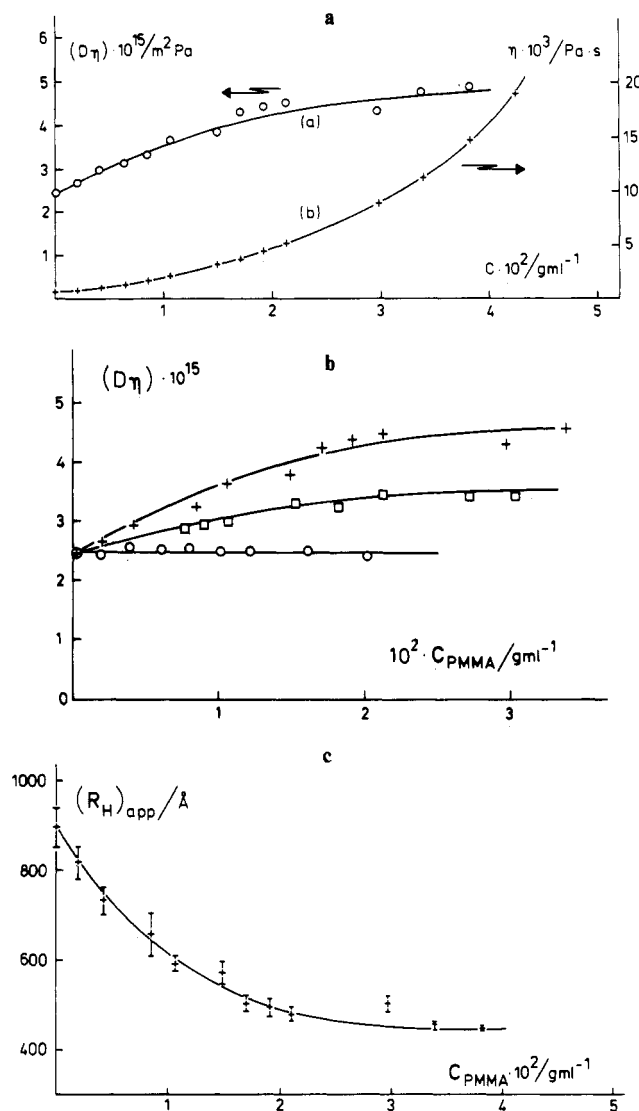


Figure 8. (a) $D_{PS}\eta$ versus C_{PMMA} , where D_{PS} refers to the self-diffusion of PS ($\bar{M}_w = 8 \times 10^6$) in solutions of PMMA ($\bar{M}_w = 4.45 \times 10^5$) in toluene with the macroscopic viscosity data indicated in the lower part of the figure. (b) $D_{PS}\eta$ versus C_{PMMA} for three molecular weights of PMMA: (+) 4.45×10^5 ; (□) 2.68×10^5 ; (○) 1.01×10^5 ; PS ($\bar{M}_w = 8 \times 10^6$). (c) Variation of the apparent hydrodynamic radius for PS (8×10^6) in solutions of PMMA (4.45×10^5) estimated by using eq 1 and the viscosity data of (a).

an effect should be more pronounced the lower the molecular weight of the guest chain and this is supported by the observation of bimodal behavior with the PS fraction with $\bar{M}_w = 1.26 \times 10^6$.

On comparison with the results of earlier investigations, we conclude that Stokes-Einstein diffusion is the primary mechanism; it is modified, however, by a coupling between the motions of the network chains and those of the probe chain. Some contribution from coil contraction cannot be excluded.

Conclusions

It is concluded that the diffusion of large particles (spheres or randomly coiled polymer chains) in semidilute solutions of a second polymer proceeds primarily via a Stokes-Einstein mechanism, i.e., the effective diffusion is determined by the macroscopic viscosity of the medium. (Reptation has earlier been considered,^{5,8,11} however, to be the dominant mechanism when the molecular weight of the test chain is substantially smaller than that of the matrix polymer or when the latter is present at a suffi-

ciently high concentration ($C > C_E$) where the coils are heavily interpenetrating.) When the guest and host polymers are of more equal size, there will be a crossover situation where both mechanisms are in evidence. This reasoning applies also to the binary polymer-solvent system, in which the participation of several diffusional modes, determined in a single experiment, has recently²³ been demonstrated. As regards the participation of fast cooperative motions (see also ref 49), we have described evidence for this in the increasing relaxation rate for the PS test chain in the PMMA network. Under favorable conditions, the network and translational motions may be separated as has earlier been noted by Nemoto et al.⁶ and Chu et al.¹³

Results that demonstrate the involvement of both network and translational motions will shortly be the subject⁵¹ of a paper dealing with the PS/cyclopentane θ system.

Acknowledgment. We are grateful to Kees de Kruif, Rijkuniversiteit te Utrecht, The Netherlands, for kindly supplying us with the sample of stearic acid stabilized silica spheres. This work was supported financially by the Swedish Natural Science Research Council.

Registry No. PS, 9003-53-6; PMMA, 9011-14-7; $(H_3C(C-H_2)_{16}CO_2H)(SiO_2)$ (graft copolymer), 112220-28-7.

References and Notes

- (1) Kuhn, R.; Cantow, H. J.; Burchard, W. *Angew. Makromol. Chem.* **1968**, *2*, 146.
- (2) Hadgraft, J.; Hyde, A. J.; Richards, R. W. *J. Chem. Soc., Faraday Trans 2* **1979**, *75*, 1495.
- (3) Cotts, D. B. *J. Polym. Sci., Polym. Phys. Ed.* **1983**, *21*, 1381.
- (4) Lodge, T. P. *Macromolecules* **1983**, *16*, 1393.
- (5) Martin, J. E. *Macromolecules* **1984**, *17*, 1279.
- (6) Nemoto, N.; Inoue, T.; Makita, Y.; Tsunashima, Y.; Kurata, M. *Macromolecules* **1985**, *18*, 2516.
- (7) Hanley, B.; Balloge, S.; Tirrell, M. *Chem. Eng. Commun.* **1983**, *24*, 93.
- (8) Martin, J. E. *Macromolecules* **1986**, *19*, 922, 1278.
- (9) Lodge, T. P.; Wheeler, L. M. *Macromolecules* **1986**, *19*, 2986.
- (10) Wheeler, L. M.; Lodge, T. P.; Hanley, B.; Tirrell, M. *Macromolecules* **1987**, *20*, 1120.
- (11) Numasawa, N.; Kuwamoto, K.; Nose, T. *Macromolecules* **1986**, *19*, 2593.
- (12) Numasawa, N.; Hamada, T.; Nose, T. *J. Polym. Sci., Polym. Phys. Ed.* **1986**, *24*, 19.
- (13) Chu, B.; Wu, D.-Q.; Liang, G.-M. *Macromolecules* **1986**, *19*, 2665.
- (14) de Gennes, P.-G. *Scaling Concepts in Polymer Physics*; Cornell University Press: Ithaca, NY, 1979.
- (15) Fujita, H.; Einaga, Y. *Polym. J.* **1985**, *17*, 1131.
- (16) Green, P. F.; Kramer, E. J. *Macromolecules* **1986**, *19*, 1108.
- (17) Bartels, C. R.; Crist, B., Jr.; Fetters, L. J.; Graessley, W. W. *Macromolecules* **1986**, *19*, 785.
- (18) Ullmann, G. S.; Ullmann, K.; Lindner, R. M.; Phillies, G. D. J. *J. Phys. Chem.* **1985**, *89*, 692.
- (19) Phillies, G. D. J.; Ullmann, G. S.; Ullmann, K. *J. Chem. Phys.* **1985**, *82*, 5242.
- (20) Brown, W. *Macromolecules* **1985**, *18*, 1713.
- (21) Brown, W.; Johnsen, R. M. *Macromolecules* **1986**, *19*, 2002.
- (22) Brown, W. *Macromolecules* **1986**, *19*, 387, 3006.
- (23) Štěpánek, P.; Koňák, C.; Jakeš, J.; Johnsen, R. M.; Brown, W. *Polym. Bull.* **1987**, *18*, 175.
- (24) Callaghan, P. T.; Pinder, D. N. *Macromolecules* **1984**, *17*, 431.
- (25) Wesson, J. A.; Noh, I.; Kitano, T.; Yu, H. *Macromolecules* **1984**, *17*, 782.
- (26) Kim, H.; Chang, T.; Yohanan, J. M.; Wang, L.; Yu, H. *Macromolecules* **1986**, *19*, 2737.
- (27) Schaefer, D. W.; Han, C. C. In *Dynamic Light Scattering*; Pecora, R., Ed.; Plenum: New York, 1985.
- (28) Lindemann, M. K. In *Polymer Handbook*; Brandrup, J.; Immergut, E. H., Ed.; Wiley: New York, 1975.
- (29) Brown, W.; Mortensen, K. *Macromolecules*, in press.
- (30) Langevin, D.; Rondelez, F. *Polymer* **1978**, *19*, 875.
- (31) Vrij, A.; Jansen, J. W.; Dhont, J. K. G.; Pathmanathan, C.; Kops-Werkhoven, M. M.; Fijnaut, H. M. *Faraday Discuss. Chem. Soc.* **1983**, *76*, 19.
- (32) Koberstein, J. T.; Picot, C.; Benoit, H. *Polymer* **1985**, *26*, 673.
- (33) Chang, L. P.; Morawetz, H. *Macromolecules* **1987**, *20*, 428.

- (34) Dautzenberg, H. *J. Polym. Sci., Polym. Symp.* **1977**, *61*, 83.
 (35) Altenberger, A. R.; Tirrell, M.; Dahler, J. S. *J. Chem. Phys.* **1986**, *84*, 5122.
 (36) von Meerwall, E. D.; Amis, E. F.; Ferry, J. D. *Macromolecules* **1985**, *18*, 260.
 (37) Miyaki, Y.; Einaga, Y.; Fujita, H. *Macromolecules* **1978**, *11*, 1180.
 (38) Phillies, G. D. J. *Macromolecules* **1987**, *20*, 558.
 (39) Brown, W.; Rymdén, R. *Macromolecules* **1986**, *19*, 2942.
 (40) Daoud, M.; de Gennes, P.-G. *J. Polym. Sci., Polym. Phys. Ed.* **1979**, *17*, 1971.
 (41) Ferry, J. D. *Viscoelastic Properties of Polymers*; Wiley: New York, 1980.
 (42) Amis, E.; Han, C. C. *Polymer* **1982**, *23*, 1042.
 (43) Wang, D. H.; Cohen, C. *Macromolecules* **1984**, *17*, 1679, 2890.
 (44) Brown, W. *Macromolecules* **1984**, *17*, 66.
 (45) Chang, T.; Yu, H. *Macromolecules* **1984**, *17*, 115.
 (46) Eisele, M.; Burchard, W. *Macromolecules* **1984**, *17*, 1636.
 (47) Huber, K.; Bantle, S.; Burchard, W.; Fetters, L. J. *Macromolecules* **1986**, *19*, 1404.
 (48) Antonietti, M.; Coutandin, J.; Sillescu, H. *Macromolecules* **1986**, *19*, 793.
 (49) Subsequent to submission of this paper, Benmouna et al.⁵⁰ have presented a theory of dynamic scattering from ternary systems as employed here. They predict two relaxation processes: cooperative (D_c) and interdiffusional (D_i) modes, where the latter refers to the relative motions of the chains. The amplitude of the cooperative mode becomes significant, however, only above a weight fraction of about 0.5.
 (50) Benmouna, M.; Benoit, H.; Duval, M.; Akcasu, Z. *Macromolecules* **1987**, *20*, 1107, 1112.
 (51) Brown, W.; Štěpánek, P. *Macromolecules*, in press.

Cyclization and Reduced Reactivity of Pendant Vinyls during the Copolymerization of Methyl Methacrylate and Ethylene Glycol Dimethacrylate

D. T. Landin and C. W. Macosko*

Department of Chemical Engineering, University of Minnesota,
 Minneapolis, Minnesota 55455. Received December 5, 1986;
 Revised Manuscript Received August 29, 1987

ABSTRACT: Methyl methacrylate was copolymerized with small amounts of ethylene glycol dimethacrylate. Monomer and pendant vinyl conversion as a function of time was measured up to the gel point. Pendant vinyl conversion was determined by ^1H NMR. Plots of pendant conversion versus monomer conversion exhibit a positive y -intercept indicating the tendency to cyclize during the formation of a primary chain. For bulk systems, this amounted to approximately 3–4% of pendant vinyls and the cyclic proportion increased with dilution. The slope of the pendant versus monomer conversion plot is attributed to the formation of cross-links and subsequent cycles. A kinetic model is developed which includes constants for cyclization and pendant reactivity. Values for these constants for the chemical systems studied are evaluated. The average pendant vinyl reactivity is found to be approximately half that of monomeric vinyl reactivity.

Introduction

Understanding the behavior of pendant vinyls is key to the study of network formation by addition polymerization involving multifunctional vinyl monomers. During such a polymerization, pendant vinyls are created when the first vinyl unit of a multifunctional vinyl monomer reacts and the group is added to a polymer chain. The pendant vinyl can then react or remain pendant. The reactivity of the pendant vinyl may be the same as that of the monomeric vinyl or it may be increased or reduced. If it reacts with a growing chain to which it is not already chemically attached, it forms a cross-link. Cyclization occurs if the pendant vinyl is already attached to the chain with which it reacts.

The behavior of pendant vinyls affects the prediction of network properties such as cross-link density, sol fraction, and critical conversion for gelation. The first theories which connected structural properties and extent of reaction were those of Flory^{1,2} and Stockmayer.^{3,4} These theories assumed equal reactivity of monomeric and pendant vinyls and all reacted pendant vinyls were cross-links (no cyclization). Walling⁵ showed that for the methyl methacrylate–ethylene glycol dimethacrylate and vinyl acetate–divinyl adipate systems there was a large discrepancy between the gel point calculated from the Flory–Stockmayer theory and that found experimentally. He attributed the discrepancy to diffusion control of the reaction. In a series of papers, Gordon and Roe⁶ disputed this explanation and instead attributed the discrepancy

Table I
Chemical Systems Investigated

system	mol % EGDMA	% dodecanethiol	vol % in tol
0N	0.00	0	100
0T	0.00	1	100
1N	0.57	0	100
2N	1.14	0	100
2N-50	1.14	0	50
2N-25	1.14	0	25
2T	1.14	1	100
3N	1.70	0	100

to the formation of cycles. There is extensive experimental evidence of the inadequacy of the Flory–Stockmayer theory for several systems.^{7–15} Two explanations for the discrepancy between observed and theoretical gel points are the formation of cycles¹⁶ and a reduced reactivity of the pendant functional group.^{14,17}

In this work, conversion of monomeric and pendant vinyls and the gel point are determined experimentally for the vinyl–divinyl system of methyl methacrylate with small amounts of ethylene glycol dimethacrylate. A simple model is proposed which includes the possibility for both cyclization and reduced reactivity. This provides a framework within which to organize and study the data.

Experimental Section

Methyl methacrylate (MMA) and ethylene glycol dimethacrylate (EGDMA) were obtained from Aldrich. MMA was washed with a 10% aqueous potassium hydroxide solution and